

## Resistive transition and magnetic field response of a Penrose-tile array of weakly coupled superconductor islands

K. N. Springer and D. J. Van Harlingen

*Department of Physics and Materials Research Laboratory, University of Illinois at Urbana-Champaign, Urbana, Illinois 61801*

(Received 14 January 1987; revised manuscript received 31 August 1987)

We have studied the effects of geometry- and magnetic-field-induced frustration on the transport properties of a Penrose-tile array of proximity-coupled superconductor islands. The arrays exhibit a broad transition to a zero-resistance state at a field-dependent critical temperature. Above this temperature, the resistance of the array modulates quasiperiodically with applied field. Measurements at different excitation levels distinguish structure arising from the irrational tile area ratio in the Penrose pattern from fine structure generated by the long-range quasiperiodic order.

It has been demonstrated that arrays of weakly coupled superconductor islands are valuable model systems for studying phase transitions, phase coherence, and frustration effects in two-dimensional systems. Most reported work has focused on regular periodic arrays of superconducting wires,<sup>1</sup> proximity-effect junctions,<sup>2-5</sup> or tunnel junctions<sup>6-8</sup> with uniform coupling between islands and a single cell area; these systems exhibit both properties of uniform high resistance or granular films, such as Kosterlitz-Thouless phase transitions, and effects resulting from long-range superconducting phase coherence, most notably magnetic-field-induced frustration. It is also possible, using thin-film microlithography techniques, to fabricate arrays with special geometric configurations, vary the coupling between islands, and introduce disorder or distortion in a controlled way. Recently, networks of narrow superconductor wires have been fabricated in a fractal Sierpinski gasket pattern<sup>9</sup> and in quasiperiodic 1D and 2D arrays;<sup>10</sup> measurements of the superconducting-normal phase boundary in these systems have yielded interesting and complex structure arising from the non-periodic but highly ordered geometry. In this paper, we report measurements of the transport properties of a two-dimensional array of superconductor islands arranged in a quasiperiodic Penrose-tile pattern. The Penrose tiling, with its fivefold long-range bond orientational order, is an important model system for studying the effects of quasiperiodicity and is the 2D analog of the quasicrystalline solids with local icosahedral symmetry. The Penrose arrays show a broad transition to a zero-resistance state when adjacent islands phase couple due to proximity-effect tunneling. In the transition region, a voltage arises from dynamical phase slips in the junction coupling associated with magnetic vortex motion. The weak coupling between islands in junction arrays enables us to study the onset of the resistance and the dynamics of the vortex excitations; this is in contrast to wire networks in which the coupling is strong except very close to the transition temperature  $T_c$ . Like the fractal<sup>9</sup> and quasiperiodic<sup>10</sup> wire networks, the Penrose array exhibits intrinsic geometric frustration—an applied magnetic field can never by itself satisfy fluxoid quantization in all cells simultaneously

since the pattern contains cells with an irrational area ratio. Therefore, circulating currents are generated, and the resulting system free energy and all array thermodynamic and dynamical properties exhibit rich and complex structure as a function of applied field.

We have studied Penrose-tile arrays of several different sizes and materials. Here we present data from our largest array, consisting of 42000 superconductor (Nb) islands arranged in a Penrose lattice on top of a normal-metal (Au) film. Figure 1 shows a small portion of the sample. The islands were formed by evaporating 1000 Å of Nb through a polymethylmethacrylate resist mask onto a 1500-Å Au film and lifting off, following ion-beam cleaning of the Au to ensure uniform metallic contact. The Penrose array was drawn by direct-write electron-beam lithography; vertices were located by projection from a five-dimensional hypercube onto a plane. Coupling between islands is through the 1.5  $\mu\text{m}$  gap in each arm of the Penrose pattern. Examination of the pattern in Fig. 1 reveals relevant features of the Penrose-tile geometry. There are two cell sizes differing in area by the golden mean  $\tau=1.618\dots$ , with more of the large cells by the

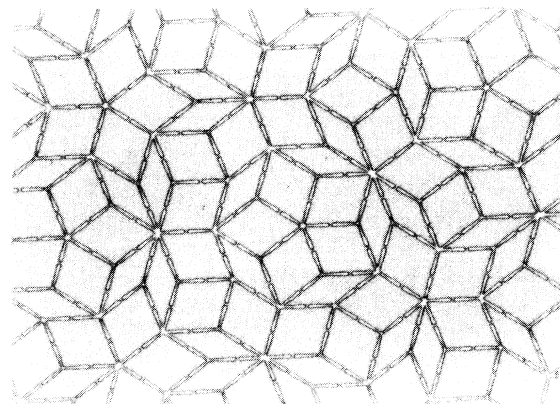


FIG. 1. Photograph of a section of the Penrose array of proximity-coupled superconducting islands. Each cell has sides of length 30  $\mu\text{m}$  and width 2  $\mu\text{m}$ ; gaps of 1.5  $\mu\text{m}$  separate adjacent islands.

same factor  $\tau$ . Each island has 3–7 bonds. The pattern exhibits no translation symmetry, but has fivefold rotation symmetry about a single vertex and local fivefold symmetric regions. Although the pattern is not self-similar, it does exhibit approximate scaling by inflation of the lattice by  $\tau^2$ .

In this paper, we report measurements of the array resistance and current-voltage characteristics as a function of temperature and applied magnetic field. Voltages across the sample are measured using an rf superconducting quantum interference device (SQUID) voltmeter with a resolution of 1 pV; resistances are measured by detecting the SQUID output voltage for an applied dc current of 10–100 nA. A transverse magnetic field, uniform to 0.1% over the sample area, is applied from a Helmholtz coil. The arrays are shielded from external magnetic fields by a superconducting Pb can and a double-nested  $\mu$ -metal can that reduces the ambient magnetic field to  $< 1$  mG.

The Penrose arrays exhibit a double resistive transition similar to that observed in periodic arrays,<sup>2–5</sup> with a sharp drop in sample resistance at the Nb transition (9.0 K) followed by a broad plateau on which the islands are superconducting but uncoupled. The resistance falls to zero at a lower temperature when phase coherence is established by proximity-effect tunneling between adjacent islands, as shown in Fig. 2(a). The temperature at which the array becomes fully superconducting and the resistance near the

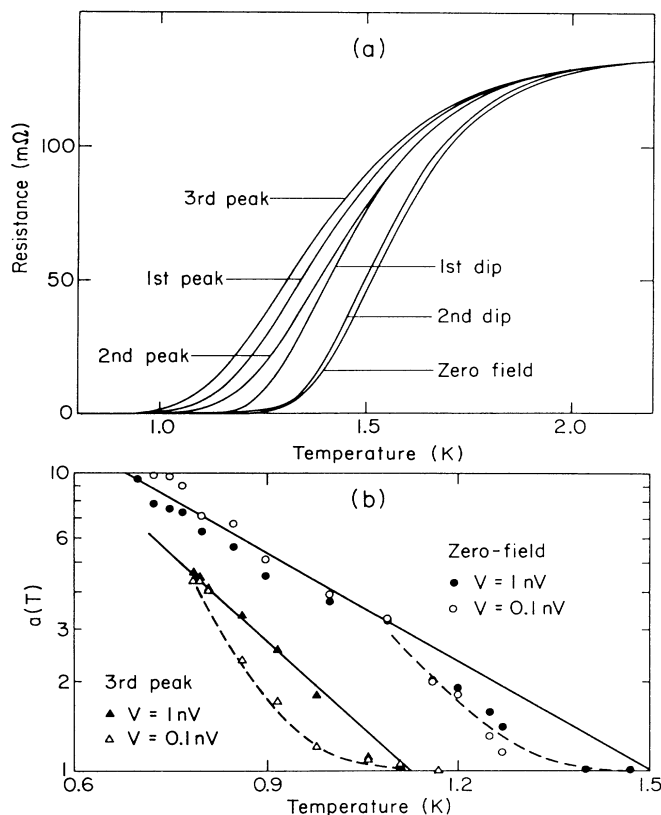


FIG. 2. (a) Resistance vs temperature for different applied magnetic fields that correspond to features in Fig. 3. (b) Current-voltage exponents vs temperature at zero field and at a field corresponding to the third peak in Fig. 3.

transition (up to about 2 K) depend strongly on the applied magnetic field; the curves in Fig. 2(a) correspond to fields at the first few peaks and dips of Fig. 3.

Previous work suggests that the resistive transition at zero applied magnetic field in periodic weakly coupled arrays<sup>2–8</sup> is a Kosterlitz-Thouless (KT) transition, characterized by an unbinding of thermally generated vortex-antivortex pairs at a critical temperature  $T_c$ . We would expect a similar result for quasiperiodic arrays since in zero field the cell geometry and arrangement should not be critical. For  $T > T_c$ , the resistance scales with the free vortex density and is predicted to be proportional to  $\exp[-A/(t - t_c)^{1/2}]$ , where  $t = k_B T/E_J(T)$  is the thermal energy normalized to the Josephson coupling energy between islands, a strongly temperature-dependent quantity in proximity arrays. In our Penrose arrays, we find that the resistance can be more accurately fit to a simple form  $\exp(-A/T)$  near  $T_c$ , suggesting a thermally activated, noninteracting free vortex density. This form has also been observed recently in tunnel junction arrays.<sup>7,8</sup> A more stringent test of KT behavior is the nonlinear  $I$ - $V$  characteristic for  $T < T_c$ ; current-induced vortex pair unbinding predicts a power-law dependence,  $V \sim I^{a(T)}$ , with  $a(T)$  exhibiting a universal jump from 1 to 3 at  $T_c$  and an increase at lower temperatures. In Fig. 2(b), we plot  $a(T)$  at zero field and at the field where the transition temperature is the lowest (about  $2.4\Phi_0$ /large cell at the third peak of Fig. 3); the exponents were determined at voltages of 1 and 0.1 nV. The  $I$ - $V$  exponents increase as the temperature is lowered, and show a change of the rate of increase at about  $a=3$  for zero field and  $a=5$  at the finite field value. Although there is no strong indication of a discontinuous jump from linear to cubic behavior, even at zero field, the observed behavior is consistent with a KT transition since for a sample of this size we expect substantial smearing. Further, determination of the low-voltage power-law exponent is complicated because these samples exhibit a real supercurrent ( $R=0$ ) state, presumably as a result of flux pinning. At finite field, there are no firm theoretical predictions for either the ground-state configuration or the nature and dynamics of the excitations.

In Fig. 3, we show an example of the nonperiodic modulation of the voltage across the array versus applied field. Phase coherence around each cell requires  $2\pi(\Phi/\Phi_0) + \sum\phi_{ij} = 2\pi n$ , where  $\phi_{ij}$  are the gauge-invariant phase

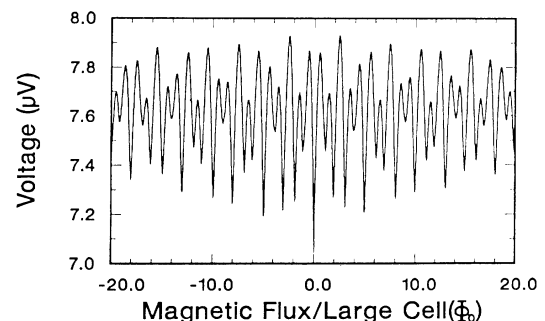


FIG. 3. Voltage vs magnetic flux/large cell for a bias current of 70  $\mu$ A and a temperature of 1.12 K.

differences between islands and  $\Phi$  is the magnetic flux in the cell, which is totally dominated by the applied field in weakly coupled arrays. In any finite field  $H$ , circulating currents produce a distribution of vortices in the ground state with an average area density  $H/\Phi_0$  and contribute to the array free energy. Dynamical properties such as the vortex flow resistance reflect the variation of the ground-state free energy and modulate with applied field.

The density of vortex excitations and the rate at which their motion induces phase slips between coupled islands play key roles in determining the structure in the magnetoresistance by setting the length scale over which the phase is correlated. A clear picture of this effect is obtained from Figs. 4(a)–4(c), which shows the measured array voltage versus flux for three different bias currents. The current both creates free vortices and drives them by the Lorentz force. The phase slip rate density is proportional to the array voltage and varies by more than three orders of magnitude over these curves. In curve (a), at high voltage, phase coherence is maintained only over short distances so that the variation of voltage with applied flux is dominated by a beating between the periodicities with field for the large and small cells. Because the large cells are more numerous by  $\tau$ , minima in the voltage roughly occur when the applied flux per large cell is an integer number of flux quanta, with the depths of the mini-

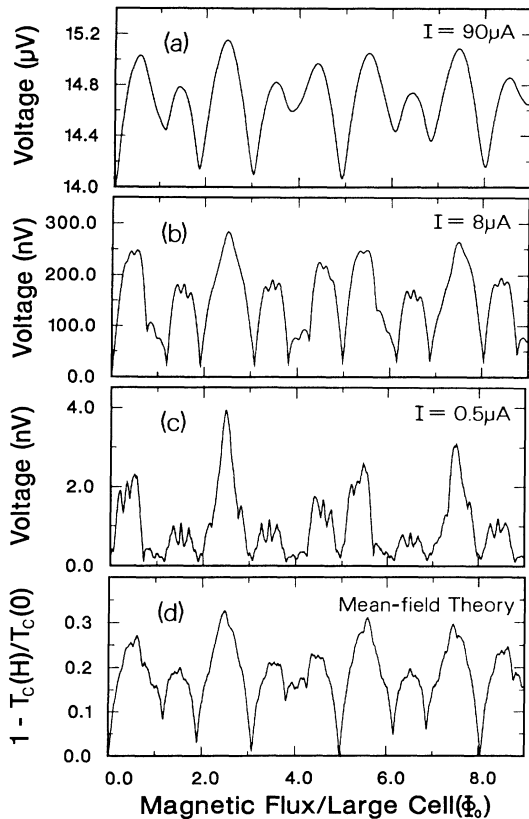


FIG. 4. Voltage vs magnetic flux/large cell for three different bias currents: (a)  $90 \mu\text{A}$ , (b)  $8 \mu\text{A}$ , and (c)  $0.5 \mu\text{A}$ . In (d), we show the result of a mean-field calculation of  $T_c$  vs magnetic flux/large cell Nori, Niu, Frandkin, and Chang.

ma modulated by the extent to which flux quantization is also satisfied by the applied field in the small cells.

As the voltage is reduced in curves (b) and (c), the relative size of features is changed dramatically and additional fine structure develops. We interpret this trend as an increase in the range over which phase coherence is important as the density of free vortex excitations and the corresponding phase slip rate decreases. This is most clearly seen by Fourier transforming the  $V$  vs  $H$  data, as in Fig. 5. The lower curve is the transform of high-voltage data, similar to Fig. 4(a); the upper curve is that of low-voltage data, intermediate between Figs. 4(b) and 4(c). Peaks indicate periodic components of the voltage with applied field arising from fluxoid quantization over different size clusters of adjacent large and small tiles. For example, a peak labeled  $(n,m)$  denotes a periodicity corresponding to  $1\Phi_0$  through an effective area composed of  $n$  large and  $m$  small cells.<sup>11</sup> In the lower (high-voltage) curve, the dominant peaks are for single large  $(1,0)$  and single small  $(0,1)$  cell areas, but nearly all integer combinations are present and can be identified in the data. In the upper (low-voltage) transform, certain area combinations are enhanced—those for which the ratio  $n/m$  (large cells/small cells) is close to  $\tau$ . The dominant peaks  $(1,0)$ ,  $(2,1)$ ,  $(3,2)$ ,  $(5,3)$ ,  $(8,5)$ ,  $(13,8)$ , . . . form a Fibonacci series of characteristic areas, although other peaks, e.g.  $(7,4)$ , whose ratios are close to  $\tau$  are also visible. These area ratios most nearly approximate the ratio of large cells to small cells in the entire Penrose pattern. This demonstrates that the configuration of ground-state vortices at these values is also quasiperiodic, matching as nearly as possible the geometry of the underlying Penrose lattice.

The mean-field calculation of the normal-superconducting phase boundary ( $T_c$  vs  $H$ ) for a Penrose lattice of

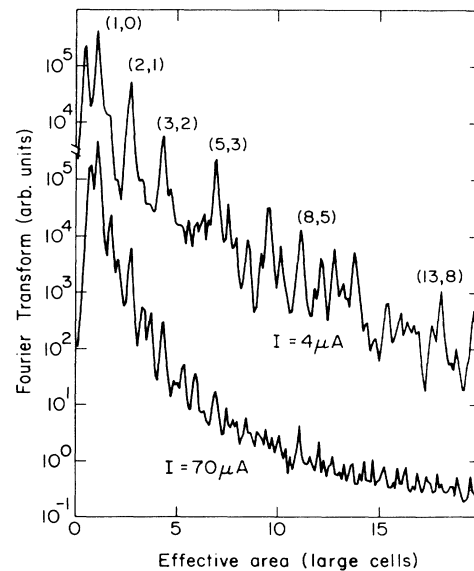


FIG. 5. Fourier transforms of the voltage vs field curves at  $T = 1.12 \text{ K}$  and bias currents of  $70$  and  $4 \mu\text{A}$ . Peaks labeled  $(n,m)$  correspond to a periodicity of  $1\Phi_0$  per area composed of  $n$  large cells and  $m$  small cells.

301 vertices by Nori, Niu, Fradkin, and Chang,<sup>12</sup> is shown for comparison in Fig. 4(d). It is in good agreement with the basic structure we observe in the magnetoresistance; deviations in the fine structure are expected due to the much smaller scale of the model lattice and to disorder (of both coupling and cell area) present in the experimental samples. In addition, these authors have studied the evolution of the structure in the superconducting phase boundary as the range of correlations between cells is increased. In agreement with our results, they find that the main peaks and dips are due to nearest-neighbor correlations, while the fine-structure characteristic of the quasiperiodicity arises from longer-range coherence.

In summary, we have observed rich structure in the magnetoresistance of a Penrose-tile array of coupled superconductor islands coming from both short-ranged geometric frustration and the long-ranged quasiperiodic topology. The voltage bias level sets the rate of vortex phase

slips, allowing us to adjust the range of the phase coherence. Resistance and current-voltage characteristics near the superconducting phase transition are consistent with a Kosterlitz-Thouless transition in zero field but show more complex behavior at finite field.

We wish to thank Jorge Gavilano, Ron Wakai, Franco Nori, and Eduardo Fradkin for many interesting discussions on arrays and quasiperiodic lattices, and Gene Hilton for development of the computer data acquisition and graphics system used in our measurements. This work was supported by the Material Research Laboratory at the University of Illinois under Grant No. NSF-DMR86-12860. We also acknowledge the University of Illinois Electron Beam Microfabrication Facility and the Microfabrication Facility of the Materials Research Laboratory.

- 
- <sup>1</sup>B. Pannetier, J. Chaussy, and R. Rammal, *J. Phys. (Paris) Lett.* **44**, L853 (1983); B. Pannetier, J. Chaussy, R. Rammal, and J. C. Villegier, *Phys. Rev. Lett.* **53**, 1845 (1984).
- <sup>2</sup>D. J. Resnick, J. C. Garland, J. T. Boyd, S. Shoemaker, and R. S. Newrock, *Phys. Rev. Lett.* **47**, 1542 (1982); R. K. Brown and J. C. Garland, *Phys. Rev. B* **33**, 7827 (1986).
- <sup>3</sup>C. J. Lobb, D. W. Abraham, M. Tinkham, and T. M. Klapwijk, *Phys. Rev. B* **26**, 5268 (1982); C. J. Lobb, D. W. Abraham, and M. Tinkham, *ibid.* **27**, 150 (1983).
- <sup>4</sup>D. Kimhi, F. Leyvraz, and D. Ariosia, *Phys. Rev. B* **29**, 1487 (1984).
- <sup>5</sup>Ch. Leeman, Ph. Lerch, G.-A. Racine, and P. Martinoli, *Phys. Rev. Lett.* **56**, 1291 (1986).
- <sup>6</sup>R. F. Voss and R. A. Webb, *Phys. Rev. B* **25**, 3446 (1982); R. A. Webb, R. F. Voss, G. Grinstein, and P. M. Horn, *Phys. Rev. Lett.* **51**, 690 (1983).
- <sup>7</sup>M. Bhushan, R. H. Cantor, J. M. Gordon, A. M. Goldman, and F. Yu, *IEEE Trans. Magn.* **MAG-23**, 1122 (1987).
- <sup>8</sup>B. J. van Wees, H. S. J. van der Zant, and J. E. Mooij, *Phys. Rev. B* **35**, 7291 (1987).
- <sup>9</sup>J. M. Gordon, A. M. Goldman, J. Maps, D. Costello, R. Tiberio, and B. Whitehead, *Phys. Rev. Lett.* **56**, 2280 (1986).
- <sup>10</sup>A. Behrooz, M. J. Burns, H. Deckman, D. Levine, B. Whitehead, and P. M. Chaikin, *Phys. Rev. Lett.* **57**, 368 (1986).
- <sup>11</sup>The indexing of the Fourier transform peaks should not be confused with the labeling of peaks in the raw magnetoresistance data by Behrooz *et al.* (Ref. 10); in their scheme ( $p, q$ ) refers to an applied magnetic field in which large cells contain  $p$  vortices and small cells  $q$  vortices.
- <sup>12</sup>F. Nori, Q. Niu, E. Fradkin, S.-J. Chang, *Phys. Rev. B* (to be published).

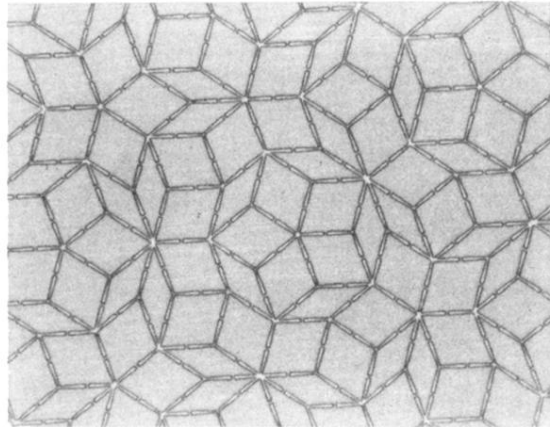


FIG. 1. Photograph of a section of the Penrose array of proximity-coupled superconducting islands. Each cell has sides of length  $30 \mu\text{m}$  and width  $2 \mu\text{m}$ ; gaps of  $1.5 \mu\text{m}$  separate adjacent islands.